Journal of Biomechanics ∎ (∎∎∎∎) ∎∎∎–∎∎∎

Contents lists available at ScienceDirect

Journal of Biomechanics

journal homepage: www.elsevier.com/locate/jbiomech
www.JBiomech.com

Stress distribution and consolidation in cartilage constituents is influenced by cyclic loading and osteoarthritic degeneration

Andrew D. Speirs [a,*], Paul E. Beaulé [b], Stephen J. Ferguson [c], Hanspeter Frei [a]

[a] Department of Mechanical and Aerospace Engineering, Carleton University, 3135 Mackenzie, 1125 Colonel By Drive, Ottawa, ON, Canada K1S 5B6
[b] Division of Orthopaedic Surgery, Ottawa Hospital, Ottawa, Canada
[c] Institute for Biomechanics, ETH Zurich, Zurich, Switzerland

ARTICLE INFO

Article history:
Accepted 17 April 2014

Keywords:
Cartilage
Bone
Osteoarthritis
Finite element analysis
Hip joint

ABSTRACT

The understanding of load support mechanisms in cartilage has evolved with computational models that better mimic the tissue ultrastructure. Fibril-reinforced poroelastic models can reproduce cartilage behaviour in a variety of test conditions and can be used to model tissue anisotropy as well as assess stress and pressure partitioning to the tissue constituents. The goal of this study was to examine the stress distribution in the fibrillar and non-fibrillar solid phase and pressure in the fluid phase of cartilage in axisymmetric models of a healthy and osteoarthritic hip joint. Material properties, based on values from the literature, were assigned to the fibrillar and poroelastic components of cartilage and cancellous and subchondral compact bone regions. A cyclic load representing walking was applied for 25 cycles. Contact stresses in the fibrillar and non-fibrillar solid phase supported less than 1% of the contact force and increased only minimally with load cycles. Simulated proteoglycan depletion increased stresses in the radial and tangential collagen fibrils, whereas fibrillation of the tangential fibrils resulted in increased compressive stress in the non-fibrillar component and tensile stress in the radial fibrils. However neither had an effect on fluid pressure. Subchondral sclerosis was found to have the largest effect, resulting in increased fluid pressure, non-fibrillar compressive stress, tangential fibril stress and greater cartilage consolidation. Subchondral bone stiffening may play an important role in the degenerative cascade and may adversely affect tissue repair and regeneration treatments.

1. Introduction

Articular cartilage can transmit large joint loads while allowing motion with very low friction. To accomplish this, the tissue has a complex multi-phase structure of water and macromolecules, primarily type II collagen and proteoglycan (Muir, 1978). Viscous and electrostatic forces between water and proteoglycan molecules impairs fluid exudation (Frank and Grodzinsky, 1987; Mow et al., 1980), resulting in elevated fluid pressures that support a substantial portion of the joint loads (Donzelli et al., 1999; Macirowski et al., 1994; Mak et al., 1987; Mow et al., 1980). This decreases the load supported by stresses in the solid component, reducing wear processes in the joint (Basalo et al., 2005). Collagen fibrils act primarily in tension, but interact with the proteoglycan network and influence the compressive properties of the tissue (Li et al., 1999; Williamson et al., 2003). Analysis of the interactions of these constituents and their role in supporting compressive loads will improve our understanding of the biomechanics of cartilage and degeneration.

Stress analysis of cartilage has evolved from early linear elastic material models (Brown et al., 1984; Hayes et al., 1972; Wei et al., 2005) to viscoelastic (Zhu et al., 1993), poroelastic (Mow et al., 1980; Wu et al., 1998) and poro-viscoelastic (Suh and Bai, 1998) to better reproduce in vitro experimental data under various loading conditions. Coupled stress-fluid flow analysis in poroelastic models can provide proteoglycan stresses and fluid pressures to study load transmission through the tissue. A transversely isotropic poroelastic model predicted regions of high stress which correspond to sites of failure, and was more sensitive to surface curvature compared to isotropic models (Donzelli et al., 1999). Fibril reinforcement of poroelastic models can also provide depth- and orientation-dependent behaviour observed in cartilage (Chegini and Ferguson, 2010; Krishnan et al., 2003; Li et al., 2009; Pierce et al., 2013a, 2013b; Wilson et al., 2004). These models better reproduce in vitro experimental results under a variety of loading conditions compared to homogeneous or isotropic models. Furthermore, separation of material behaviour to mimic tissue ultrastructure in computational models allows analysis of stresses within the different cartilage constituents (Chegini and Ferguson,

* Corresponding author. Tel.: +1 613 520 5089; fax: +1 613 520 5715.
E-mail address: andrew.speirs@carleton.ca (A.D. Speirs).

http://dx.doi.org/10.1016/j.jbiomech.2014.04.031
0021-9290/

2010; Li et al., 2009). However analyses using fibril-reinforcement have been mostly limited to models representing cartilage plugs or cartilage regions with low curvature (Chegini and Ferguson, 2010; Li et al., 2009; Mononen et al., 2011). Donzelli et al. (1999) showed that increased curvature shifts the location of peak stress from the cartilage surface to the cartilage-bone interface, as well as away from the centre of contact compared to planar surfaces.

Thus the goal of this study was to analyse stress and pressure in a poroelastic, fibril-reinforced cartilage model in the highly curved hip joint. The role in load support of the fibrillar and poroelastic components was examined by comparing stress and pressure in a healthy joint, as well as changes in load sharing with cyclic loading. The influence of typical osteoarthritic degenerative changes in the periarticular tissues on load sharing between cartilage constituents and consolidation was examined by simulating proteoglycan depletion, collagen fibrillation and subchondral sclerosis.

2. Methods

A generic axisymmetric hip joint model was created (Fig. 1). All analyses were performed in Abaqus (v6.10, Dassault Systèmes) using the non-linear solver to account for contact and finite strain formulations. The femoral head subchondral bone surface was arbitrarily based on a sphere of 26 mm and the acetabular subchondral surface had a radius 2.5 mm larger (Anderson et al., 2010). The femoral and acetabular cartilage layers were 1 mm thick, similar to cartilage on the superior femoral head (Athanasiou et al., 1994) resulting in a minor incongruity at the periphery (Menschik, 1997; Neusel et al., 1996). Cartilage regions were modelled with bi-linear poroelastic elements (CAX4P). Each cartilage region consisted of 25 elements in the depth direction and 800 elements in the tangential direction. The subchondral compact bone layer was 2 mm thick and consisted of bi-linear elements (CAX4). The cancellous regions consisted of both four and three node linear elements (CAX3 and CAX4).

2.1. Material models

An elastic modulus of 1.37 GPa was assigned to compact bone regions (Brown and Vrahas, 1984) and 247 MPa to the cancellous regions (Brown et al., 2002). The cartilage layers were modelled as a fibril-reinforced poroelastic material (Chegini and Ferguson, 2010) with properties based on data reported from the human femoral head. In a poroelastic model, the solid and fluid phases are assumed to be incompressible. Thus any macroscopic compression of the tissue results in changes in the pore volume only and requires outflow of the fluid. The fluid flow is impeded by fluid-solid interactions such as viscous shear and hydrostatic forces, measured by the permeability. The poroelastic non-fibrillar component, simulating proteoglycan and water, was governed by the modulus (E), Poisson's ratio (ν) and permeability (k), which were assumed to be uniform and isotropic. For the initial "healthy" model, $E=1.64$ MPa and $\nu=0.3$ (Démarteau et al., 2006). Poisson's ratio was calculated from the relationship between elastic and aggregate moduli since the observed Poisson's ratio is influenced by the collagen fibrils (Chegini and Ferguson, 2010).

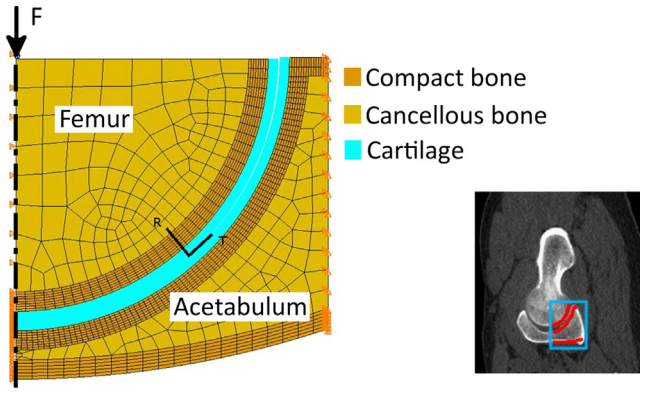

Fig. 1. The generic axisymmetric model of the hip was based on the cross section in the oblique sagittal slice of a computed tomography scan, outlined in blue (right). The compact bone layers are highlighted in red. The material properties were assigned for each region identified. A time-varying cyclic force, F, was applied to the femoral head. Fibril preferred stiffness directions are defined relative to the locally radial (R) and tangential (T) directions of the cartilage tissue shown by the black lines (left). (For interpretation of the references to color in this figure legend, the reader is referred to the web version of this article.)

Permeability decreases exponentially with cartilage consolidation (Lai et al., 1981). A permeability–void ratio relationship was determined from data reported for femoral head cartilage (Démarteau et al., 2006; Li et al., 1999):

$$k = 1.06\times10^{-17}\exp\{2.0e\}$$

where e is the void ratio. For an initial void ratio of 2.7, i.e. water content of 73% (Démarteau et al., 2006), the permeability in the unloaded state was 2.3×10^{-15} m^4/N s.

The fibrillar component was modelled with a strain- and depth-dependent, tensile-only modulus defined in a user subroutine (UMAT). Mesh regions were created for the fibrillar component with the same mesh density as the poroelastic component. The tensile-only strain-dependent modulus of the tangential fibrils was calculated at each material point (Korhonen et al., 2003):

$$E_t = s(1.0\varepsilon_t + 190) \quad \text{for} \quad \varepsilon_t > 0$$

where ε_t is the strain in the tangential direction and s is a scale factor. The scale factor was 1.0 at the bearing surface to provide maximum tensile stiffness tangent to the surface. It decreased linearly to 0.38 at the tidemark to simulate the preferred fibril orienation such that fibril stiffness in the tangential direction at the tidemark was reduced by 62% (Chegini and Ferguson, 2010; Verteramo and Seedhom, 2004). For compressive strains, the modulus was arbitrarily set to 0.00001 MPa to improve solver convergence. Comparable data was not available for radial fibrils. However, since fibril density is approximately the same in deep and superficial zones, a similar continuum model was implemented for radial fibrils. The modulus was calculated from the radial strain and linearly scaled from 100% stiffness at the tidemark to 38% at the bearing surface. These were applied as tangent moduli to increment the fibril stress from the strain increment. It was assumed that all off-diagonal shear terms of the fibril stress tensor were zero.

2.2. Constraints

Due to identical mesh geometry, the nodes of the fibril mesh regions were coincided with and displacements were constrained to the nodes of the underlying poroelastic regions. Adjacent mesh regions were fully constrained along the common boundary (TIE constraint) and the cartilage/bone boundary was impermeable. Contact at the bearing surfaces was modelled with a non-linear penalty formulation. Free draining of open cartilage surfaces was implemented with an adaptive seepage algorithm in a user subroutine (FLOW) to create a more physiological boundary condition (Federico et al., 2004; Ferguson et al., 2000; Pawaskar et al., 2010; Warner et al., 2001). A surface material point was closed if the contact stress at the closest surface node was greater than zero, or open otherwise. Seepage from an open surface maintained the surface pore pressure close to zero simulating a free-draining boundary condition.

2.3. Loading and boundary conditions

All nodes at the outer edge of the acetabulum were constrained to have no displacement in the vertical or horizontal directions. The hip contact force was applied through a single node on the symmetry axis which was kinematically coupled to all nodes on the upper bone surface of the femur region.

The hip contact force was applied to the femur to simulate normal walking. The time-varying force measured in a patient over a 1.04 s gait cycle was applied, which varied from 266 N to 2072 N (31–241% of body weight) (Bergmann et al., 2001). The load profile was repeated for 25 cycles.

2.4. Simulation of degeneration

In order to investigate the role of degenerative changes in peri-articular tissues in the hip model, associated changes in properties were applied. Proteoglycan depletion and collagen fibrillation (Muir, 1978) and increased subchondral bone density i.e. sclerosis (Kellgren and Lawrence, 1957; Tonnis, 1976) have been reported in osteoarthritic joints. Four different models were used to investigate the effects of changes in the biomechanical properties of periarticular tissues. Each model is described relative to the healthy reference model:

1. Proteoglycan depletion: the poroelastic modulus (E) was decreased by 15% for moderate degeneration. Permeability (k) was correspondingly increased by 20% (Armstrong and Mow, 1982).
2. Fibrillation: due to a lack of reference data, the modulus (E_t) of the tangential fibrils was arbitrarily decreased by 50% from the calculated value while the modulus of the radial fibrils was not modified.
3. Subchondral sclerosis: the modulus of all bone regions was increased by 50%, corresponding to differences predicted by bone mineral density changes in the hip (Speirs et al., 2013).

Please cite this article as: Speirs, A.D., et al., Stress distribution and consolidation in cartilage constituents is influenced by cyclic loading and osteoarthritic degeneration. Journal of Biomechanics (2014), http://dx.doi.org/10.1016/j.jbiomech.2014.04.031